

## Interface for the Factor-inclusion Weighting Approach in Determining the Number of Multipath Propagation Clusters

Marielle Anne Roque and Lawrence Materum

Electronics and Communications Engineering Department, De La Salle University, Philippines

marielle\_roque@dlsu.edu.ph



### ABSTRACT

Design and development of MIMO communication systems require a comprehensive analysis of channel characteristics. In real-world applications, the channel consists of randomly propagating signals that travel in two or more paths called multipaths. Literature shows an approach of analyzing the channel, which is knowing the number of clusters or groupings of these multipaths. This paper presents a development of an interface featuring a factor weighing approach in determining the number of clusters. Different visualizations and evaluation results are shown in the interface that allows users to visually compare and analyze the proposed method. Further, the paper shows the consistency of the results since it matches the analysis of the novel approach proposed by the authors.

**Key words:** Graphical User Interface, User Interface, Clustering Methods, Multipath Channels, Radio Wave Propagation, Channel Models.

### 1. INTRODUCTION

In communication systems, one effective technique to communicate in a faster and reliable transmission is the use of a multiple-input multiple-output (MIMO) system. In this type of system, multiple transmitter (Tx) and receiver (Rx) antennas are used to carry data for optimal performance and range aiming high-speed links with good quality-of-service. For developing and designing a MIMO system, a comprehensive analysis of the channel is needed, the medium through which propagated signal travels. With multiple propagated signals reaching the receiver by two or more paths, each of the paths is called multipath or multipath component (MPC). Analysis of these MPCs presents multipath clustering or the tendency of MPCs to form groupings called multipath clusters [1], [2]. A reference like [3] analyzed channel models visually through generated plots. Studies such as [4], [5] also used plots with parameters of delay, azimuth, and elevation from the receiver or mobile station. In knowing the number of clusters, these studies analyze the multipaths visually and group them subjectively. The studies were more focused on the effect of clustering and number of clusters to the system. This approach would provide inaccuracy for describing the channel due to the lack of computation for the optimum number of cluster fit for the channel.

In this paper, an interface is developed for a factor-inclusion weighting approach in determining the number of clusters [6]. The approach is an effective method in determining the number of clusters by assigning different weights for CVIs, algorithms in determining the number of clusters. Graphical user interfaces (GUIs) is one of the past decades important technological developments, mainly in the field of information technology. Aside from improvements in hardware, portraying the information has greatly improved for users, especially those visually impaired using GUIs. A GUI is a useful tool such that it makes the most of the capacity of the user's sight. Aiming the capability of a person's sight to take in much information, GUIs allow the person to control the information flow on what is relevant and discard what is not [7]. Examples of UIs that were developed in the authors' department can be found in [8–17][9–12], [18–21]. Certain of them, however, lack some analysis platform [22], [23], unlike those in [24–32]. In this work, using a GUI, the user of this interface can analyze a MIMO channel visually with its multipaths, calculated clusters, and cluster count.

Section II of this paper discusses the flow of how the interface was done, whereas Section III presents the achieved results and explanations, and lastly Section IV highlights the essential findings and summary of the work.

### 2. METHODOLOGY

#### 2.1 Implementation

Interaction between the data and user happens when selecting and acting at positions in the display in a graphical user interface. An excellent graphical user interface guides the user with the graphical content and the user's intent [33]. MATLAB is the language used in this paper such that it can generate an interactive GUI. This GUI is a software application maximizing the point-and-click control to eliminates the time and necessity to learn and type commands in a language to run the application. The code follows the step-by-step process of the approach in [6]. Codes were created or programmed rather than using a GUI development environment of MATLAB for more control over the design and development of the interface. This undertaking included the properties and behaviors of objects existing in the interface.

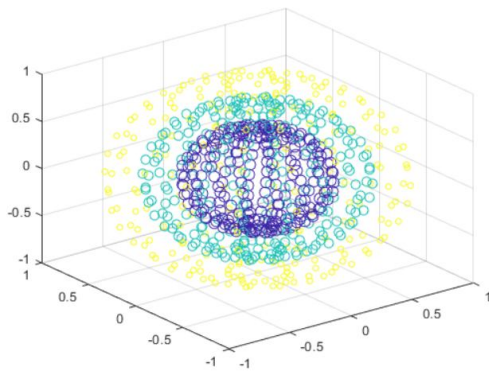


**Figure 1:** Sample visual 3-D plot in MATLAB [39]

### 2.1.1 COST 2100 Channel Data Generation

Most interactive interfaces require user input to be read as initial data. In this study, exhausting propagating wave properties of a wireless multipath channel from COST 2100 was first done. Channel model COST 2100 is a stochastic model that generates properties of MIMO channels over time, frequency, and space. This model reflects reality such as the global delay and angular spreads, which was statistically proven to be reliable and consistent as obtained from channel sounding experiments and measurement validations [34–36]. An updated version of a Matlab code by [37] implementing COST 2100 channel was used with additional codes to translate into Excel spreadsheet format. Unlike in [6] where an indoor hall scenario was only accounted for, this study lets the user choose from four different scenarios by varying the following external parameters:

- Type of network: Indoor Hall or Semi-Urban
- Type of Link: Single or Multiple
- Type of Scenario: LOS or NLOS

A tab would be developed only focusing the original data from COST 2100. Exhausted data from the model are the important MPC parameters such as the delay( $\tau$ ) and azimuth( $\phi$ ) and co-elevation( $\theta$ ) angle of departure (AOD) and angle of arrival (AOA) distances [38]. With the COST 2100 using directional channels, a table was placed in this tab to show the exhausted multipaths and their respective MPC parameters. This was done by using *uitable* function of MATLAB. The interface also showed informative parameters of the channel model such as all path power relative to the LOS path ( $P_l$ ), reference cluster IDs of each path ( $I_{ref}$ ), Position of MS and BS, frequency and velocity of MS. With the data recorded, visual plots were also a feature added in this tab to visually view the generated data using *scatter3* function of MATLAB. Figure 1 is a sample of a 3-D scatter plot of MATLAB. Colors of the scatter plot can be used to portray the relative power of each multipath.

### 2.1.2 Data Transformation

Following the steps of [6], the extracted dataset  $X$  from COST 2100 proceeded with matrix transformations due to the distance measure restriction of algorithms involved. Angular data (azimuth and elevation) of  $X$  was transformed into directional cosines  $X_T$  to provide a linear scale for the pre-processing. This interface would show the effect of transforming the data by visually plotting the multipaths again but with transformed parameters. Each multipath data can be tracked from a table placed in the tab.  $X_T$  was expected to result with a total of 7 parameters accounting both the departure and arrival of each path. The whitening transformation was then processed to obtain normalized data,  $X_w$ , having different units of measure to lessen biasing to a parameter during clustering. A comparison of the data pre-processing technique would all be placed in one tab.

### 2.1.3 Multipath Clustering

With clusters being considered in the channel, clustering algorithms have been provided to resort extensive dataset channels. These algorithms evaluate the relationships among patterns such that it would organize these patterns into groups, or clusters. KPower-means algorithm is an automatic and improved partitioning clustering method [38] that adapts cluster power as a weight of grouping multipaths into  $K$  clusters. The advantage of KPower-means to other clustering algorithms is its ability to remove weak components that are not significant in the channel.

The first step of KPower-means required defining the value of  $K$  which is the maximum number of multipath clusters. MATLAB is capable of inserting a text box in the interface where the user can input value using the 'edit-box' style of function *icontrol*. This tool was used so the interface could generate groupings of the existing multipaths from the read desired number of clusters. The data to be clustered were the whitened data set. Visual plots were also placed in a tab specifically for this section.

### 2.1.4 Determining Number of Multipath Clusters

Cluster validity indices (CVIs) are used for evaluating the resulting clusters of clustering algorithms and for providing analysis on identifying the clusters. Practically, having no prior information of the reference number of clusters, internal CVI is used that determines how well the results of a cluster analysis fit the data without reference to any external information.

For this study, Calinski-Harabasz (CH) [40], Kim-Park (KP) [41] and Silhouette (SI) [42] indices were used to analyze the intrinsic properties of each cluster found in the whitened dataset,  $X_w$ . These indices used to compare the partition with intrinsic properties of a cluster,  $C_k$ . The method of weighting of CVIs was based on [6] to achieve a better

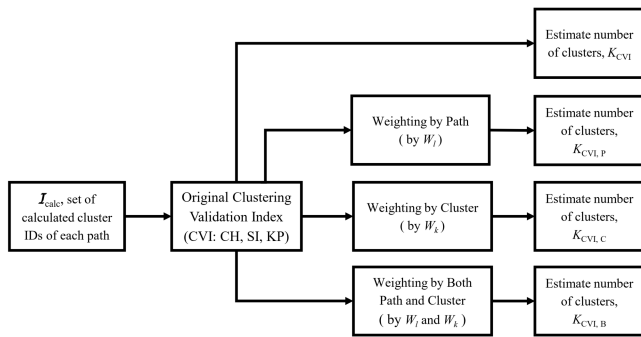


**Figure 2:** Flow Diagram of Different Weighting Approach in each CVI

determination of cluster count. Figure 2 portrays the various weightings used.

There were three approaches of weighting for each validity index labeled as weighting by path, weighting by cluster, and weighting both by cluster and by path. Each of these approaches differs on how to integrate the weights to the algorithm of the indices. Weighting by path,  $CVI_P$ , include using  $W_l$  which can be  $P_l, \tau_l, \phi_l^{AOD}, \phi_l^{AOA}, \theta_l^{AOD}, \theta_l^{AOA}$ , and  $v_l$ . However, weighting by cluster,  $CVI_C$ , used parameters taken from a cluster,  $W_k$ .  $W_k$  can be  $P_k, \bar{S}_\tau, \bar{S}_{\phi^{AOD}}, \bar{S}_{\phi^{AOA}}, \bar{S}_{\theta^{AOD}}, \bar{S}_{\theta^{AOA}}$ , and  $\bar{S}_v$ . The third approach of weighting,  $CVI_B$  incorporated both  $W_l$  and  $W_k$ . Thus, there were 21 weighting methods used depending on what weight involved and approach of weighting presented in Figure 2.

**2.2 Evaluation**

This section provides the details on how the interface shows validation of implementing the factor-inclusion weighting approach. Tabs for this section would be provided in the interface to show tests if the used approach would be better than the original CVIs.

**2.2.1 Analysis of Clustering Algorithm using External CVIs**

To evaluate the performance of KPower-means clustering algorithm. It is compared to the extracted reference grouping from COST 2100. The interface would show a confusion matrix to show the similarity or difference of the grouping. The confusion matrix,  $\zeta$ , comprises:

- $\zeta_{TP}$  = True Positive (the path is correctly assigned to its reference cluster)

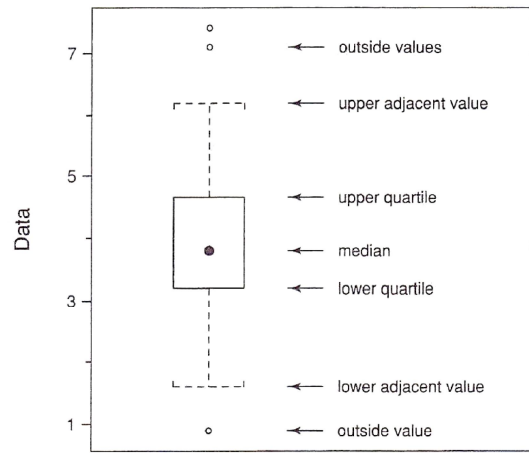


**Figure 3:** Tukey box plot [43]

- $\zeta_{TN}$  = True Negative (the path is correctly determined that it does not belong to other reference clusters)
  - $\zeta_{FP}$  = False Positive (the path is incorrectly assigned to its reference cluster)
  - $\zeta_{FN}$  = False Negative (the path is incorrectly determined that it does not belong to other reference clusters)
- External validity indices are measures of comparison. Used

$$\xi_E = -\sum_k \frac{|C_k|}{L_{(k)}} \log \left( \frac{|C_k|}{L_{(k)}} \right) \tag{1}$$

external validity indices were Entropy, Jaccard, Rand, and Purity indices.

Entropy,  $\xi_E$ , measures how the various multipaths are distributed within each cluster [44].

where  $|C_k|$  is the total path count in the cluster  $k$ .

$$\xi_P(I_{ref}, I_{calc}) = \frac{1}{L_{k_{ref}}} \sum_{k_{calc}} \max |C_{k_{calc}} \cap C_{k_{ref}}| \tag{2}$$

Purity  $\xi_P$  measures the extent of similarity of the grouping of multipaths by the clustering algorithm and the reference grouping [44]. The terminology can be derived from entropy where the computation of the purity of the calculated cluster is given by:

Rand index  $\xi_R$  considers equally false positives and false negatives. Thus, the weight of a path being wrongly clustered with a dissimilar path is mathematically equal when a path is incorrectly not grouped with a similar path

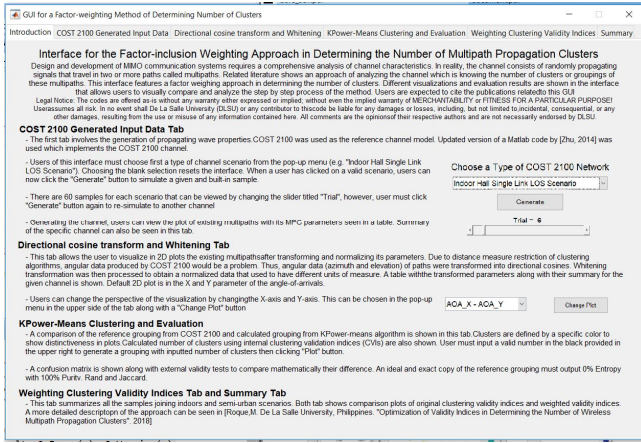


Figure 4: Screenshot of the 'Introduction' Tab

[12]. Jaccard index, however, does not consider whether a path is incorrectly assigned to its reference cluster [45].

$$\xi_R = \frac{\zeta_{TP} + \zeta_{TN}}{\zeta_{TP} + \zeta_{TN} + \zeta_{FP} + \zeta_{FN}} \quad (3)$$

$$\xi_J = \frac{\zeta_{TP}}{\zeta_{TP} + \zeta_{FP} + \zeta_{FN}} \quad (4)$$

### 2.2.2 Cluster Analysis and Robustness Test using Sensitivity measure and Relative Uncertainty measure

Accuracy and precision for determining the number of clusters are essential features that must be computed and analyzed. In this study, relative uncertainty,  $J$ , was used as a measure of the accuracy of the calculated number of clusters to the reference number of clusters. The inputs were  $K_{ref}$  the reference number of clusters in a snapshot generated by COST 2100 and  $K_{calc}$ , the calculated number of clusters. An ideal and desired value of relative uncertainty is close to 0%. Equation 5 defines the calculation of relative uncertainty. Changes in the relative uncertainty from using the original method of determining number clusters to using weighted clustering validity indices would indicate the performance of the proposed solution.

$$J = |K_{calc} / K_{ref} - 1| \quad (5)$$

The interface would show graphs presented in a Tukey box plot to display a summary of distribution. This plot is done by using the function *boxplot* of MATLAB. It portrays the sample mean and the sample standard deviation by plotting symbols and interval bars to represent the inter-quartile range. The median is the center location of the distribution represented by a dot, as shown in Figure 3. Upper and lower quartile distance of the inter-quartile range measures the spread of the distribution by the relative distances of the data from the median. Adjacent values, on the other hand, present

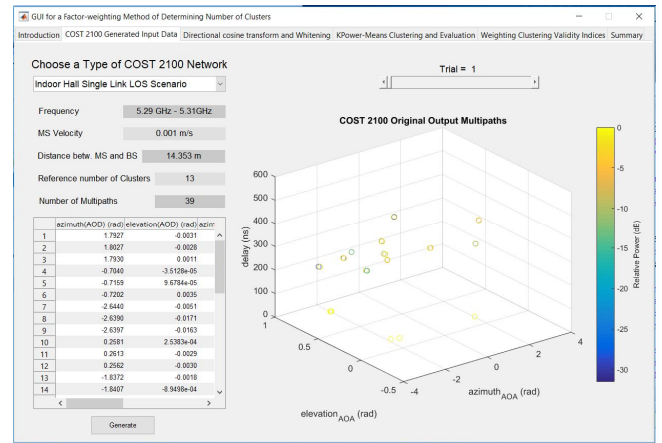


Figure 5: Screenshot of the 'COST 2100 Generated Input Data' Tab in operation

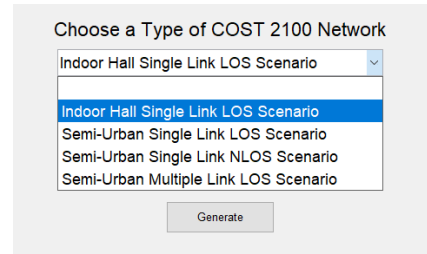
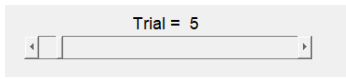


Figure 6: User input of the type of COST 2100 channel scenario

the spread and shape information for the tails of the distribution. The upper adjacent value represents the largest observation greater than or equal to the sum of the upper quartile and 1.5 times the inter-quartile range. Lower adjacent value is the smallest observation less than or equal to the difference of the lower quartile and 1.5 times the inter-quartile range. Outliers, which are the unusually large or small observations, are also seen in a Tukey box plot represented by extreme values [43]. This plot would be useful for providing a fair comparison of distributions such as the evaluation of each validation indices in every trial of methodology process.

For the robustness test, the performance behavior of the algorithms used for clustering and determining the number of clusters can be quantified by seeking a variation of the output based on given inputs. One of the simple and most used sensitivity measures is the first-order sensitivity index obtained by Sobol method [46]. This measure can be graphed in the last part of the interface to summarize the overall performance of the factor-inclusion weighting approach.



**Figure 7:** Slider feature for choosing the channel to be analyzed in all parts of the interface

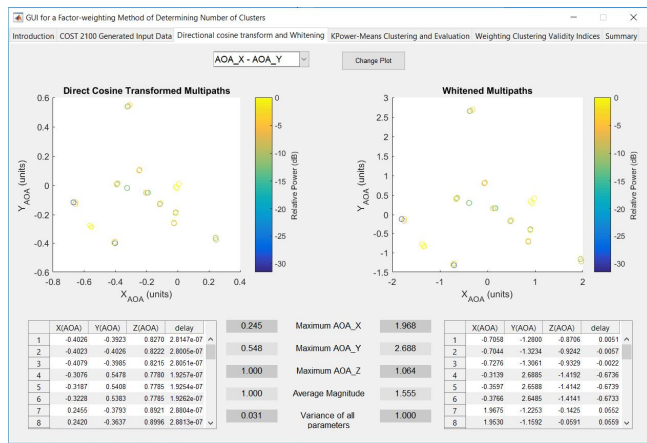


**Figure 8:** Screenshot of 'Directional cosine transform and Whitening' Tab

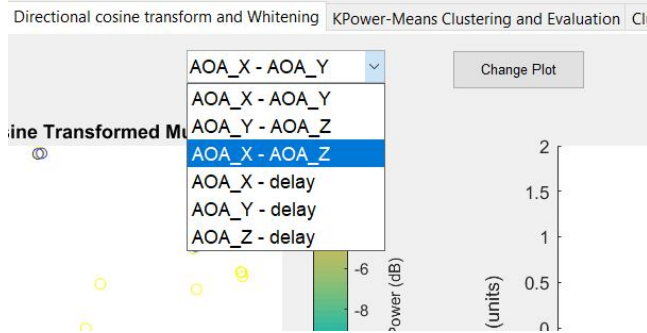


**Figure 9:** Different perspective of graphing multipaths

### 3. RESULTS AND DISCUSSIONS

Figure 4 shows the first tab that gives details about the interface. Subsections below describe the results of each tab after running the interface

#### 3.1 COST 2100 Generated Input Data Tab

This section presents and discusses the features of the 'COST 2100 Generated Input Data' tab. Figure 5 shows the screenshot of the tab in operation. The interface allows users to one-by-one visualize and analyze a built-in channel sample taken from COST 2100. As seen in Figure 6, there were four different types of scenarios considered in this

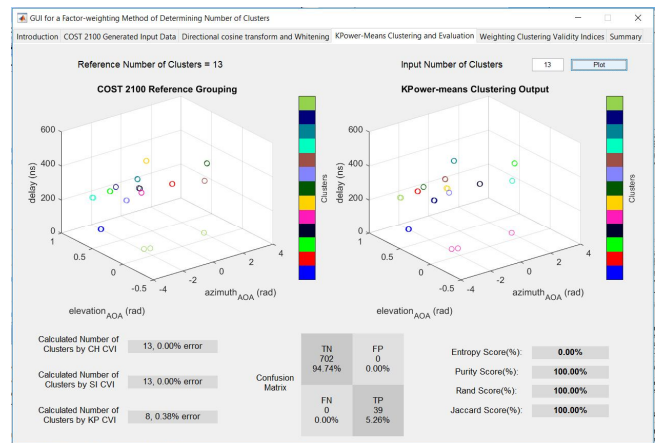


**Figure 10:** COST 2100 generated reference groupings

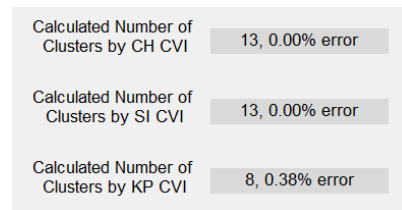


**Figure 11:** Approaches in calculating the number of clusters

interface. Users of this interface can choose from the pop-up menu a type of channel scenario to be generated in the interface (e.g., "Indoor Hall Single Link LOS Scenario"). Choosing the blank selection resets the interface. When a user has clicked on a valid scenario; the user is now able to click the "Generate" button to simulate a given and built-in sample.

There are sixty samples for each scenario that can be viewed in this interface. A slider titled "Trial" allows the user to generate one of these, as seen in Figure 7. The user, however, must click the "Generate" button again to resimulate another channel after changing the Trial slider.

The channel after generating it to the interface is visualized through scatter plots. Users can view the plot of existing multipaths with its MPC parameters seen in a table. A summary of the specific channel properties can also be seen in this tab. Color of each point follows the color bar indicating the power of the cluster.

Comparisons of the channel scenarios can be analyzed by generating all the built-in channel scenarios one-by-one. The relative power of the multipaths in a semi-urban scenario can range to a minimum much smaller to that in an indoor. The number of multipaths and clusters were obviously different in each channel scenario such that a semi-urban

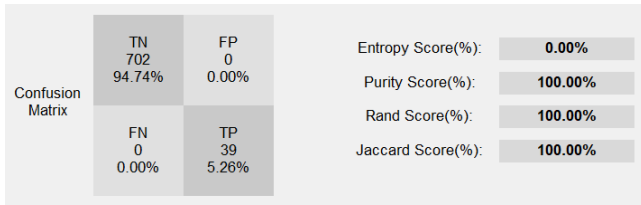


Figure 12: Approaches in calculating the number of clusters

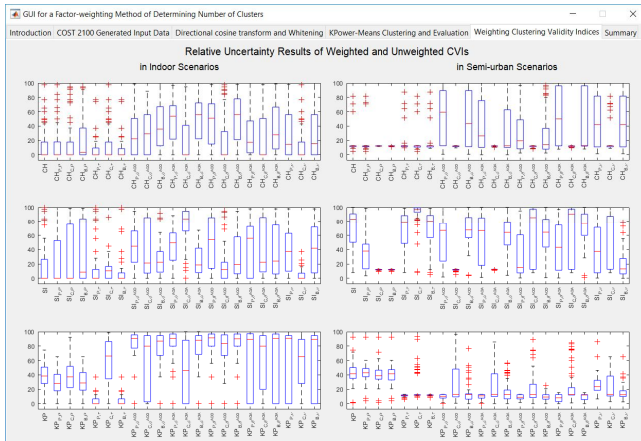


Figure 13: Screenshot of the 'Weighting Clustering Validity Indices' Tab

environment is a bigger network in size, thus, more multipaths. Meanwhile, in an indoor scenario, the delay and frequency are smaller compared to a semi-urban.

### 3.2 Directional cosine transform and Whitening Tab

A screenshot of this tab is seen in Figure 8. This tab allows the user to visualize in 2D plots the existing multipaths after transforming and normalizing its parameters. A table listing the transformed parameters along with their summary for the given channel is a feature of this tab. Default 2D plot is in the X and Y parameter of the angle-of-arrivals. Comparing the table shown in the 'COST 2100 Generated Input Data' Tab in Fig. 5, and the tables are shown in Fig. 8, there were more columns in the tables in this tab. Thus, the number of dimensions to be clustered were more than the reference multipath parameters. This situation led to a verification that processing directional cosine transformation to the data provides more dimensions for clustering.

Users can also visually see in the lower part of the tab the comparison between before and after whitening the data. The uneven distribution of the parameters before whitening can be seen when analyzing the values in the table and also the scatter plot. Users can change the perspective of the visualization by changing the X-axis and Y-axis point. This change can be chosen in the pop-up menu, as seen in Figure

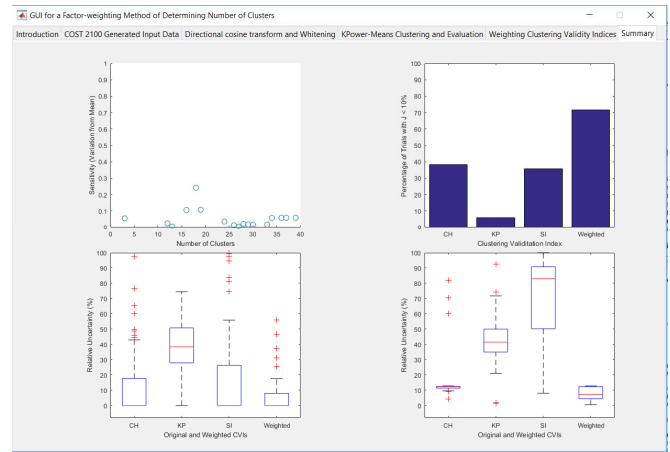


Figure 14: Screenshot of the 'Summary' Tab

9 in the upper side of the tab along with a "Change Plot" button. Whitening the data allowed the variance of all parameters to be one as seen in all the channel samples.

### 3.3 KPower-Means Clustering and Evaluation Tab

This tab focuses on the clustering approach used in the interface. The reference grouping of the multipaths was taken from the COST 2100 simulations before using the channel sample in the interface. With the focus of the interface being weighting approaches, a comparison of the reference grouping from COST 2100 and calculated grouping from KPower-means algorithm is shown in this tab.

For graphing, the user must input a valid number in the blank text-box provided in the upper right to generate a grouping with inputted number of clusters then clicking the "Plot" button as seen in Figure 10. Clusters are still defined by a specific color to show their distinction from one another in the scatter plots.

The problem that can be observed in using the clustering method was knowing the optimal number of clusters when the reference number of clusters is practically not given in network design. Since KPower-means needed the number of clusters as an input, a method called internal validity indices (CVIs) are used to calculate the number of clusters based on Approaches in calculating the number of clusters that CVI's criteria. Users can refer and use the calculated number of clusters using these CVIs. However, this calculated number of clusters was seen to sometimes be unequal from the reference number of clusters. Thus, the user can also see in this tab the relative uncertainty error of the cluster counts.

For evaluation of the generated clusters by KPower-means algorithm, a confusion matrix is shown along with external validity tests to compare its difference or similarity mathematically from the reference clustering as seen in

Figure 12. An ideal and exact copy of the reference grouping must output 0% Entropy with 100% Purity, Rand, and Jaccard.

From different iterations seen in the confusion matrix for different channel sample, it can be observed that the value of true negatives (paths correctly determined to not belong with each other) is the dominant effect of the performance of the clustering algorithm.

### 3.4 Weighting Clustering Validity Indices Tab

This section discusses the tab that summarizes all the samples joining indoors and semi-urban scenarios. Figure 13 shows the screenshot of the 'Weighting Clustering Validity Indices' Tab. The tab shows visualizations of comparing different methods of determining the cluster count based on its relative uncertainty error. The methods to be compared in the plots compare performances were the original and weighted CH, KP, and SI indices.

The internal validity indices are very different from each other based on the comparison of indoor and semi-urban scenarios. Best results seen among original CVIs are by using the Calinski-Harabasz index in both indoors and semi-urban. However, knowing the number of clusters is easier for original CVIs in indoors than outdoors such that their medians were along with the 0% relative uncertainty. There are still several outliers that calculated the number of clusters very far from the reference number of clusters. Also, the results can be said to be imprecise when the box representing the distribution had a large height in indoors whereas, for semi-urban scenarios, the results of relative uncertainties in Calinski-Harabasz were more precise.

Weighting the CVIs results that not all weights and approach of adding the weight improved the performance of determining the number of clusters. The successful weighting of indices for an indoor hall scenario was concluded to use weighting by path and weighting simultaneously within and between clusters using *delay* and weighting by cluster using *Doppler spread* in CH and SI indices. Meanwhile, power weighting using all approaches improved Kim-Park index; however, not enough as their relative uncertainty values rely on a distribution with a mean and median larger than 10%. Therefore, in an indoor scenario, CH and SI indices improved when the indices considered the delay of each path in a cluster while differentiating the Doppler spread of each cluster. For semi-urban scenarios, different weights improved the performance of the original indices as some of them decreased the mean and median of relative uncertainty distribution. However, the only weighting that passed the desirable less than 10% relative uncertainty was weighting with *azimuth and elevation angle of departure and arrival* using weighting by path and weighting simultaneously within and between clusters. Thus, the angular spread was more distinct in a semi-urban scenario.

### 3.5 Summary Tab

Joining the indoor and semi-urban scenarios and also all the valid and successful weighting of the CVIs, comparison plots of original clustering validity indices and weighted validity indices are shown. The valid and successful weighting of CVIs were those approaches that resulted in less 10% mean and median relative uncertainty. Visually, the calculated number of clusters from the weighted index was more accurate and precise than the original indices.

For the test of robustness, the plot for sensitivity analysis was taken across the number of reference clusters. Testing the robustness of the weighted index, a small value of sensitivity index meant that the relative uncertainty is not far from the mean relative uncertainty of all the scenario. Thus, from the graph, the relative uncertainty does not rely exceptionally on the number of clusters.

## 4. CONCLUSION

The interface was made for users to obtain the results by letting them choose the type of scenario, then generating a sample of this scenario. Users are also allowed to choose other simulation of the scenario such that the interface holds sixty samples for each scenario. Each tab was informative in portraying the step-by-step process of a factor-inclusion weighting approach in determining the cluster count. The performance results of the factor-inclusion weighting coincide with the original results in [6]. The effective weight in indoors was found to be the delay, whereas, for semi-urban scenarios, by angular data.

## ACKNOWLEDGMENT

The authors would like to thank DOST and DLSU for supporting this research.

## REFERENCES

- [1] A. Goldsmith, *Wireless Communications*. Cambridge University Press, 2005.  
<https://doi.org/10.1017/CBO9780511841224>
- [2] A. F. Molisch, *Wireless communications*. John Wiley & Sons, 2005.
- [3] A. A. M. Saleh and R. Valenzuela, "A Statistical Model for Indoor Multipath Propagation," *IEEE J. Sel. Areas Commun.*, vol. 5, no. 2, pp. 128–137, 1987.  
<https://doi.org/10.1109/JSAC.1987.1146527>
- [4] Z. Tang and A. S. Mohan, "Impact of Clustering in Indoor MIMO Propagation Using a Hybrid Channel Model," *EURASIP J. Appl. Signal Process*, 2004.  
<https://doi.org/10.1155/ASP.2005.1698>
- [5] N. Czink, M. Herdin, H. Ozelik, and E. Bonek, "Number of multipath clusters in indoor MIMO propagation environments," *Electron. Lett.*, vol. 40, no. 23, pp. 1498–1499, 2004.  
<https://doi.org/10.1049/el:20046570>

- [6] M. A. Roque and L. Materum, "Determination of the Number of Multipath Clusters in Indoor Wireless MIMO Systems at 5.3 GHz," (*accepted for publication*).
- [7] A. D. N. Edwards, "ITD Journal: The Rise of The Graphical User Interface," *Itd.athenpro.org*. 2018.
- [8] A. D. M. Africa and J. S. Velasco, "Development of a urine strip analyzer using artificial neural network using an android phone," *ARNP J. Eng. Appl. Sci.*, vol. 12, no. 6, pp. 1706–1713, 2017.
- [9] A. M. Don Africa, "A rough set-based expert system for diagnosing information system communication networks," *Int. J. Inf. Commun. Technol.*, vol. 11, no. 4, pp. 496–512, 2017.  
<https://doi.org/10.1504/IJICT.2017.10008315>
- [10] A. D. M. Africa, "A mathematical fuzzy logic control systems model using rough set theory for robot applications," *J. Telecommun., Electron., Comput. Eng.*, vol. 9, no. 2–8, pp. 7–11, 2017.
- [11] A. D. M. Africa, "A logic scoring of preference algorithm using ISO/IEC 25010:2011 for open source web applications moodle and wordpress," *ARNP J. Eng. Appl. Sci.*, vol. 13, no. 15, pp. 4567–4571, 2018.
- [12] P. J. M. Loresco and A. D. Africa, "ECG print-out features extraction using spatial-oriented image processing techniques," *J. Telecommun., Electron., Comput. Eng.*, vol. 10, no. 1–5, pp. 15–20, 2018.
- [13] R. C. Gustilo and E. P. Dadios, "Machine vision support system for monitoring water quality in a small scale tiger prawn aquaculture," *J. Adv. Computat. Intell. Intell. Informat.*, vol. 20, no. 1, pp. 111–116, 2016.  
<https://doi.org/10.20965/jaciii.2016.p0111>
- [14] A. M. D. Celebre, A. Z. D. Dubouzet, I. B. A. Medina, A. N. M. Surposa, and R. C. Gustilo, "Home automation using raspberry Pi through Siri enabled mobile devices," *8th Int. Conf. Human., Nanotechnol., Inf. Technol., Commun. Control, Env. Manag., HNICEM 2015*, 2016.  
<https://doi.org/10.1109/HNICEM.2015.7393270>
- [15] J. Del Espiritu, G. Rolluqui, and R. C. Gustilo, "Neural network based partial fingerprint recognition as support for forensics," *8th Int. Conf. Human., Nanotechnol., Inf. Technol., Commun. Control, Env. Manag., HNICEM 2015*, 2016.  
<https://doi.org/10.1109/HNICEM.2015.7393227>
- [16] N. J. C. Libatique, G. L. Tangonan, R. Gustilo, W. K. G. Seah, C. Pineda, M. L. Guico, G. Abrajano, R. Ching, J. L. Zamora, A. Espinosa, A. C. Valera, R. Lamac, H. Dy, J. Pusta, E. M. Trono, A. Gimpaya, J. R. S. Luis, S. J. Gonzales, and A. T. Lotho, "Design of a tropical rain - Disaster alarm system: A new approach based on wireless sensor networks and acoustic rain rate measurements," *IEEE Instrum. Meas. Technol. Conf. (I2MTC)*, pp. 1341–1345, 2009.  
<https://doi.org/10.1109/IMTC.2009.5168663>
- [17] K. J. D. A. Virtudez and R. C. Gustilo, "FPGA implementation of a one-way hash function utilizing HL11-1111 nonlinear digital to analog converter," *Proc. IEEE Reg. 10 Annu. Int. Conf. (TENCON)*, 2012.  
<https://doi.org/10.1109/TENCON.2012.6412237>
- [18] R. C. Gustilo and E. P. Dadios, "Behavioural response analysis using vision engineering (BRAVENet)," *J. Adv. Computat. Intell. Intell. Informat.*, vol. 21, no. 2, pp. 211–220, 2017.  
<https://doi.org/10.20965/jaciii.2017.p0211>
- [19] R. A. M. Cruz, N. D. S. Enero, E. F. Samonte, R. C. Gustilo, and G. Arada, "Design of optimal thermoelectric generator array for harnessing electrical power from air-conditioning unit," *Int. J. Eng. Technol.(UAE)*, vol. 7, no. 4, pp. 238–241, 2018.
- [20] H. C. Dy and R. C. Gustilo, "Characterization of signal response for surface water movements in underwater optical wireless communications," *Proc. IEEE Reg. 10 Annu. Int. Conf. (TENCON)*, 2012.
- [21] L. Villanueva and R. C. Gustilo, "Artificial neural network based antenna sensitivity assignments for chaotic Internet Service Provider network architecture," *Int. J. Eng. Technol.(UAE)*, vol. 7, no. 2, pp. 14–17, 2018.  
<https://doi.org/10.14419/ijet.v7i2.3.9958>
- [22] S. Chatvichienchai and Y. Kawasaki, "Spreaddb: Spreadsheet-based user interface for querying and updating data of external databases," *Int. J. Adv. Trends Comput. Sci. Eng.*, vol. 7, no. 2, pp. 6–10, 2018.  
<https://doi.org/10.30534/ijatse/2018/01722018>
- [23] L. Vladareanu, V. Vladareanu, H. Yu, H. Wang, and F. Smarandache, "Robot advanced intellectual control developed through flexible intelligent portable platform," *Int. J. Adv. Trends Comput. Sci. Eng.*, vol. 8, no. 1, 2019.
- [24] M. K. Cabatuan, E. P. Dadios, and R. N. G. Naguib, "Computer vision-based breast self-examination palpation pressure level classification using artificial neural networks and wavelet transforms," *Proc. IEEE Reg. 10 Annu. Int. Conf. (TENCON)*, 2012.  
<https://doi.org/10.1109/TENCON.2012.6412282>
- [25] M. N. Eman, M. K. Cabatuan, E. P. Dadios, and L. A. G. Lim, "Detecting and tracking female breasts using neural network in real-time," *Proc. IEEE Reg. 10 Annu. Int. Conf. (TENCON)*, 2013.  
<https://doi.org/10.1109/TENCON.2013.6718899>
- [26] J. A. C. Jose, M. K. Cabatuan, E. P. Dadios, and L. A. Gan Lim, "Depth estimation in monocular Breast Self-Examination image sequence using optical flow," *Int. Conf. Human., Nanotechnol., Inf. Technol., Commun. Control, Env. Manag. (7th HNICEM) joint with 6th Int. Symp. on Adv. Computat. Intell. Intell. Informat., co-located with 10th ERDT Conf.*, 2014.  
<https://doi.org/10.1109/HNICEM.2014.7016220>
- [27] J. A. C. Jose, M. K. Cabatuan, E. P. Dadios, and L. A. G. Lim, "Stroke position classification in breast self-examination using parallel neural network and wavelet transform," *Proc. IEEE Reg. 10 Annu. Int. Conf. (TENCON)*, vol. 2015-January, 2015.  
<https://doi.org/10.1109/TENCON.2014.7022288>
- [28] J. A. C. Jose, M. K. Cabatuan, R. K. Billones, E. P. Dadios, and L. A. G. Lim, "Monocular depth level estimation for breast self-examination (BSE) using RGBD BSE dataset," *Proc. IEEE Reg. 10 Annu. Int. Conf. (TENCON)*, vol. 2016-January, 2016.  
<https://doi.org/10.1109/TENCON.2015.7372948>
- [29] R. A. A. Masilang, M. K. Cabatuan, and E. P. Dadios,

- “Hand initialization and tracking using a modified KLT tracker for a computer vision-based breast self-examination system,” *Int. Conf. Human., Nanotechnol., Inf. Technol., Commun. Control, Env. Manag., (7th HNICEM) Joint with 6th Int. Symp. Adv. Computat. Intell. Intell. Informat., co-located with 10th ERDT Conf.*, 2014.
- [30] R. A. A. Masilang, M. K. Cabatuan, E. P. Dadios, and L. G. Lim, “Computer-aided BSE torso tracking algorithm using neural networks, contours, and edge features,” *Proc. IEEE Reg. 10 Annu. Int. Conf. (TENCON)*, vol. 2015-January, 2015.
- [31] E. Mohammadi, E. P. Dadios, L. A. Gan Lim, M. K. Cabatuan, R. N. G. Naguib, J. M. C. Avila, and A. Oikonomou, “Real-time evaluation of breast self-examination using computer vision,” *Int. J. Biomed. Imag.*, vol. 2014, 2014.
- [32] S. L. Rabano, M. K. Cabatuan, E. Sybingco, E. P. Dadios, and E. J. Calilung, “Common garbage classification using MobileNet,” *Proc. 10th Int. Conf. Human., Nanotechnol., Inf. Technol., Commun. Control, Env. Manag. (HNICEM)*, pp. 1–4, Nov. 2018.  
<https://doi.org/10.1109/HNICEM.2018.8666300>
- [33] D. L. Hecht, “Printed embedded data graphical user interfaces,” *Computer*, vol. 34, no. 3, pp. 47–55, Mar. 2001.
- [34] R. Verdone and A. Zanella, *Pervasive mobile and ambient wireless communications*. Springer, 2012.
- [35] L. Liu, C. Oestges, J. Poutanen, K. Haneda, P. Vainikainen, F. Quitin, F. Tufvesson, and P. Doncker, “The COST 2100 MIMO channel model,” *IEEE Wireless Commun.*, vol. 19, no. 6, pp. 92–99, 2012.  
<https://doi.org/10.1109/MWC.2012.6393523>
- [36] L. M. Correia, “Wrapping Up and Looking at the Future,” in *Pervasive Mobile and Ambient Wireless Communications: COST Action 2100*, R. Verdone and A. Zanella, Eds. London: Springer London, 2012, pp. 661–671.
- [37] M. Zhu, *COST 2100 channel model Matlab code*. GPL, 2014.
- [38] N. Czink, “The Random-Cluster Model – A Stochastic MIMO Channel Model for Broadband Wireless Communication Systems of the 3rd Generation and Beyond,” Vienna University of Technology, 2007.
- [39] I. The MathWorks, “3-D scatter plot,” *Mathworks.com*. 2017.
- [40] T. Calinski and J. Harabasz, “A dendrite method for cluster analysis,” *Commun. Stats.*, vol. 3, no. 1, pp. 1–27, 1974.
- [41] K. Do-Jong, P. Yong-Woon, and K.-J. Park, “A Novel Validity Index for Determination of the Optimal Number of Clusters,” *IEICE Trans. Inf. Syst., D*, vol. 84, no. 2, pp. 281–285, Feb. 2001.
- [42] P. J. Rousseeuw, “Silhouettes: A graphical aid to the interpretation and validation of cluster analysis,” *J. Computat. Appl. Math.*, vol. 20, pp. 53–65, 1987.  
[https://doi.org/10.1016/0377-0427\(87\)90125-7](https://doi.org/10.1016/0377-0427(87)90125-7)
- [43] W. S. Cleveland, *The Elements of Graphing Data*. AT&T Bell Laboratories, 1994.
- [44] C. Manning, P. Raghavan, and H. Schütze, *Introduction to Information Retrieval*. Cambridge University Press, 2008.  
<https://doi.org/10.1017/CBO9780511809071>
- [45] B. Desgraupes, *Clustering Indices*. University Paris Ouest, 2013.
- [46] I. M. Sobol, “Sensitivity estimates for nonlinear mathematical models,” 1993.